ISSN 1063-7761, Journal of Experimental and Theoretical Physics, 2019, Vol. 128, No. 5, pp. 754–760. © Pleiades Publishing, Inc., 2019.
Russian Text © The Author(s), 2019, published in Zhurnal Eksperimental'noi i Teoreticheskoi Fiziki, 2019, Vol. 155, No. 5, pp. 886–893.

ORDER, DISORDER, AND PHASE TRANSITION IN CONDENSED SYSTEM

Fractal Dimension Effect on the Magnetization Curves of Exchange-Coupled Clusters of Magnetic Nanoparticles

S. V. Komogortsev[a], R. S. Iskhakov[a], and V. A. Fel'k[b,*]

[a] *Kirensky Institute of Physics, Federal Research Center Krasnoyarsk Scientific Center, Siberian Branch, Russian Academy of Sciences, Krasnoyarsk, 660036 Russia*

[b] *Reshetnev Siberian State University of Science and Technology, Krasnoyarsk, 660049 Russia*

**e-mail: vlaf80@mail.ru*

Received September 29, 2018; revised December 6, 2018; accepted December 6, 2018

Abstract—The effect of the fractal dimension of exchange-coupled clusters of magnetic nanoparticles on their magnetization curves is predicted by scaling estimates. These predictions form the basis for the experimental technique used for determining the fractal dimension of nanoparticle clusters from the magnetization curves. We estimate the reliability of determining the dimension by such methods with the help of micromagnetic simulation. It is shown that the effective dimension of magnetic correlation volumes, which is determined from analysis of the magnetization approaching saturation, is in conformity with the dimension of fractal clusters determined from analysis of their morphology. The dimension estimated from analysis of the coercive field on the particle size in a physically natural situation of the dipole–dipole interaction between nanoparticles provides estimates of the cluster dimension, which strongly differs from estimates obtained from analysis of their morphology.

DOI: 10.1134/S1063776119040095

1. INTRODUCTION

The properties of a system substantially depend on its dimensionality. The dimensionality can be topological, metric, or fractal. These dimensions are used in physical theories in different manners and are measured in different ways. Here, we consider the manifestation of the fractal dimension in magnetic properties of nanomaterials and the possibility of its reliable measurement using these properties.

A fractal is usually interpreted as a structure consisting of self-similar substructures repeated on decreasingly small scales [1, 2]. Deterministic fractals (e.g., Sierpinski's carpet) are well known. Such fractal structures have been recently considered for applications in micro- and nanoelectronics [3, 4]. Stochastic fractal structures are observed most often in nature where scaling should be considered statistically [1, 2, 5, 6]. In the physics of condensed media, there are numerous examples of fractal structures (polymers, colloidal aggregates, porous media, rough surfaces, spin configurations in dilute magnets, etc.) [7–10]. Fractal dimension can be measured experimentally by direct methods based on microscopic processing of images as well as in small-angle scattering experiments with neutrons, X-rays, or scattered light [2, 5, 6, 11, 12]. In recent decades, the effect of fractal dimension in magnetic correlation volumes on the magnetization curves and ferromagnetic resonance in amorphous and nanostructured materials has been considered [13–18]. This effect was predicted using scaling considerations in the random magnetic anisotropy model [15, 19, 20]. In integer-dimensional nanostructured materials, the reliability of such predictions has been confirmed in experiments [14, 21–25]. On the other hand, quantitative relations between the dimension and the magnetization curve have been used for experimental determination of fractal dimension from magnetization curves in various nanostructured magnetic materials [26–28]. The noninteger dimension was estimated using the law of approach to magnetic saturation (LAMS) in granular magnetic films in the vicinity of the percolation threshold, as well as nanoporous magnetic media [26, 27]. The rigorous micromagnetic theory of magnetization curves in nanomagnets with arbitrary dimension d of magnetic correlation volumes or with dimension of magnetic anisotropy nonuniformities exists only for systems with integer dimension $d = 1, 2, 3$ [29–33]; therefore, the possibility of reliable measurement of fractal dimension from the magnetization curves requires separate investigation. In this paper, the possibility of such measurements is demonstrated using micromagnetic calculations.

2. THEORETICAL BACKGROUND

The magnetic microstructure of a material consisting of exchange-coupled nanoparticles with randomly oriented axes is an aggregate of stochastic magnetic

domains or magnetic correlation volumes containing a large number of nanoparticles [34]. The anisotropy constant of a magnetic correlation volume is $\langle K\rangle = K/\sqrt{N}$, where N is the number of nanoparticles in the volume and K is the magnetic anisotropy constant of an individual nanoparticle. The number N can be estimated as $N = (l_m/l_g)^d$, where l_m is the magnetic correlation length, l_g is the grain (nanoparticle, crystallite) size, and d is the fractal dimension of the magnetic correlation volume. Using these estimates and the results obtained for dependence $l_m = f(l_g, H)$ [15, 35], we can obtain dependence $\langle K\rangle = f(l_g, H)$ of average anisotropy of the magnetic correlation volume on the grain size and on the external magnetic field. Such a description explains the dependence of coercive field $H_c \propto l_g^6$ observed in bulk nanocrystalline alloys [21]. Stochastic magnetic domains or magnetic correlation volumes are observed in nanocrystalline alloys [36–39]. In moderate and high fields, the magnetic microstructure is transformed into a magnetization ripple that assumes the form of slight periodic variations of the magnetization direction due to fluctuating local easy magnetization axis [40–42]. Quantities l_m and $\langle K\rangle$ for a weak applied field are given in terms of the random anisotropy model for $l_g < \delta$:

$$l_m \propto \delta^{4/(4-d)}/l_g^{d/(4-d)}, \quad (1)$$

$$\langle K\rangle \propto K(l_g/\delta)^{2d/(4-d)}, \quad (2)$$

where $\delta = \sqrt{A/K}$. Here, A is the exchange constant.

The exponents in Eqs. (1) and (2) depend on the fractal dimension of the magnetic structure. According to formula (2), the coercive field depends on the grain size as

$$H_c \propto \langle K\rangle \propto l_g^{2d/(4-d)},$$

In the experiment, the fractal dimension can be estimated from the exponent in power law $H_c(l_g)$. This possibility has already been used for interpreting some experiments [24, 30, 43, 44].

In an amorphous or nanocrystalline ferromagnet, the LAMS is determined by normalized dispersion (ν_m) of the magnetization unit vector component $\mathbf{m}_{tr}(\mathbf{x}) = \mathbf{M}_{tr}(\mathbf{x})/M_s$ transverse to the field (here, M_s is the saturation magnetization):

$$M(H) = M_s(1 - \nu_m(H)). \quad (3)$$

The theory for the LAMS including d was proposed in [29]. In the approach used in [29], dimension d is equal to the multiplicity of the integral used for calculating $\nu_m(H)$. Therefore, the noninteger dimension was excluded in that case. It was shown later that the fractal dimension in the LAMS can be attributed to the dimension of the nonuniformity of the local easy magnetization axis as well as to the fractal dimension of the magnetic correlation volume [14, 15, 22].

The scaling approach to magnetic correlation volumes (see Eq. (1)) naturally presumes the possibility of a noninteger (fractal) dimension. The magnetization in an ensemble of magnetic correlation volumes can be assumed to be statistically independent [15]. In this case, the magnetization dispersion in expression (3) can be estimated as

$$\nu_m = (a\langle K\rangle/(M_s H))^2,$$

where $a = \sqrt{1/15}$ for the uniaxial symmetry and $a = \sqrt{2/105}$ for the cubic symmetry of the local magnetic anisotropy. As a result, the following expression was proposed for normalized dispersion [45]:

$$\nu_m(H) = \frac{a^2}{\delta^4}\frac{l_H^4}{1 + (l_H/l_g)^d} = \frac{(aH_a)^2}{H^{(4-d)/2}(H^{d/2} + H_{ex}^{d/2})}. \quad (4)$$

Here, $H_a = 2K/M_s$ is the local magnetic anisotropy field, $H_{ex} = 2A/(M_s l_g^2)$ is the exchange field, and $l_H = \sqrt{2A/(M_s H)}$ is the magnetic correlation length in fields $H \ll H_{ex}$. It should be noted that l_H in this limit acquires physical meaning ($l_H \gg l_g$). There exists a transition between two power-law regimes located above and below H_{ex}:

$$\nu_m(H) = (aH_a)^2 \begin{cases} H^{-2}, & H \gg H_{ex}, \\ H^{-(4-d)/2} H_{ex}^{-d/2}, & H \ll H_{ex}. \end{cases} \quad (5)$$

In logarithmic axes, these regimes correspond to two linear segments with different slopes of the $\nu_m(H)$ curve [15, 46]. The measurement of the exponent appearing in relation (5) for $H \ll H_{ex}$ can also be used for estimating d. Since there is no rigorous micromagnetic theory for noninteger fractal dimension, the validity of scaling estimated (2) and (5) will be verified with the help of micromagnetic simulation. The rigorous micromagnetic theory of magnetization curves for structures with integer dimension of magnetic anisotropy nonuniformities, which was mentioned in Introduction, was developed for a continuous medium disregarding the dipole–dipole interaction. In measuring practice, this disregard can be justified with an appropriate choice of the sample shape and the magnetic field orientation. In materials consisting of clusters with complex morphology, the dipole–dipole interaction can substantially affect their properties; for this reason, the present work is also aimed at the verification of the effect of the dipole–dipole interaction on the results of determination of fractal dimension using expressions (2) and (5).

3. NUMERICAL EXPERIMENT

Two-dimensional fractal clusters for micromagnetic calculations were obtained using the diffusion-limited aggregation (DLA) model in the Visions of Chaos v.59.3 package [47]. The DLA clusters contain-

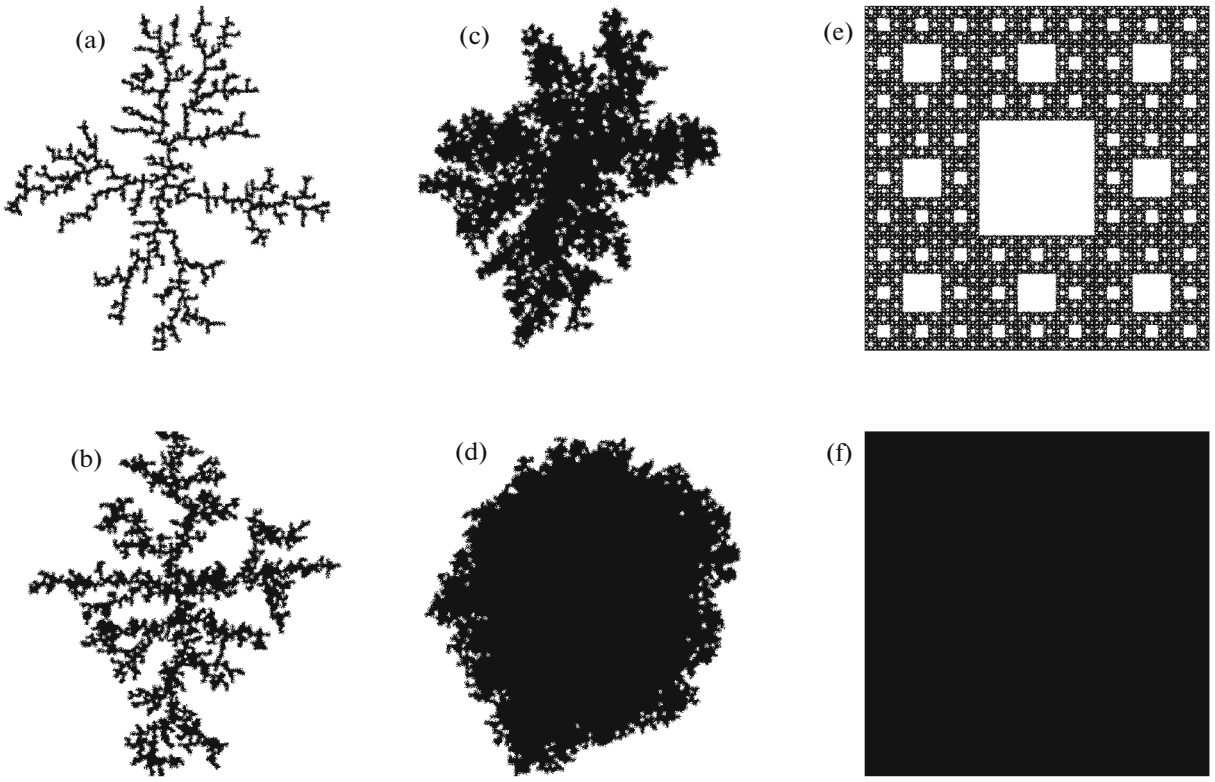

Fig. 1. Clusters used for micromagnetic calculations: (a–d) DLA clusters; (a) DLA cluster grown with particle adhesion probability $p = 1$; (b) $p = 0.1$; (c) $p = 0.01$; and (d) $p = 0.001$; (e) cluster with the Sierpinski carpet structure; (f) solid-state film element.

ing from 2×10^4 to 7×10^4 particles differing in their adhesion probability have different dimensionalities, which were determined by the box counting (BC) method [1, 2, 6] (Fig. 1). In addition, we have studied the fractal cluster in the form of the Sierpinski carpet, dimension $d = \ln 8/\ln 3 \approx 1.89$ of which is well known. Micromagnetic simulation of a fractal cluster was performed using the OOMMF package [48]. Cluster images were used as a mask for the micromagnetic problem in which pixels filled with black color corresponded to a magnetization of 8.6×10^5 A/m; the remaining pixels corresponded to zero magnetization.

Cell size l_g was chosen equal to a layer thickness of 5 nm. Since we are interested in the magnetic properties of an ensemble of one-domain nanoparticles, the cell size corresponds to one pixel of the mask. Therefore, the magnetization of a particle in the cluster is uniform. The local uniaxial magnetic anisotropy constant of each cell was $K = 10^5$ J/m^3. The easy magnetization axes of particles were oriented at random. Positive exchange constant A was chosen in the range from 0.25×0^{-11} J/m to 2×10^{-11} J/m to ensure various ratios of competing exchange energy to anisotropy energy. It should be noted that the dimensionless ratio of these energies can be expressed in terms of ratio l_g/δ of the characteristic scales as $Kl_g^2/A = (l_g/\delta)^2$ [49, 50]; for this reason, further results will be given as functions of l_g/δ.

4. RESULTS AND DISCUSSION

To verify the applicability of Eqs. (2) and (5) for measuring the fractal dimension of clusters, we have calculated the maximal hysteresis loop accentuating its reversible segment corresponding to the approach to the saturation magnetization in the range of fields much stronger than the coercive field (Fig. 2). In the range of fields comparable with the coercive field, magnetization correlations spread over scales much larger than the particle size (Fig. 3). Therefore, the mean magnetic anisotropy energy of the magnetic correlation volume must contain information about the structure of exchange-coupled cluster within the given scale.

The change of asymptotic dependence from $M_s - M(H) \propto H^{-\alpha}$ to $M_s - M(H) \propto H^{-2}$ in LAMS, which is predicted by expression (5), can be treated as a change of exponent $\alpha(H)$ in empirical expression

$$M_s - M(H) \propto H^{-\alpha},$$

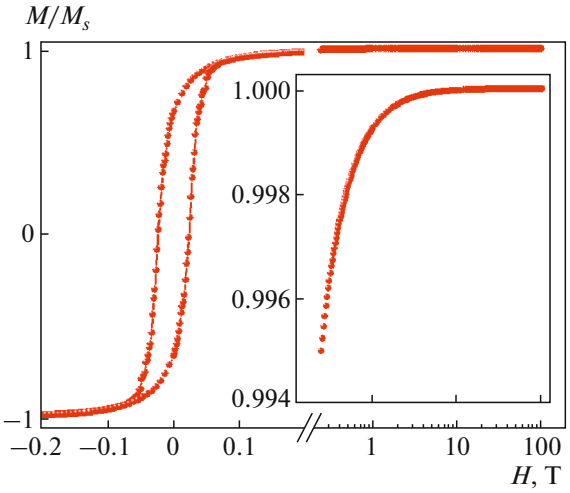

Fig. 2. (Color online) Hysteresis loop for a fractal cluster (DLA cluster *a*). The inset shows the region of approach to saturation magnetization.

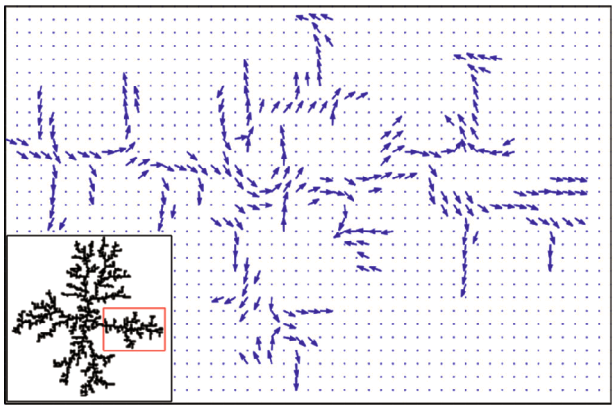

Fig. 3. (Color online) Micromagnetic structure in one of the branches for DLA cluster *a* (see inset) in the state with $M/M_s = 0$ and $H = H_c$.

describing a small segment of the $M(H)$ curve in the vicinity of a certain field H. Such an approach was used earlier in the analysis of a theoretical expression for the LAMS in thin magnetic films [51] and in the experimental data processing [45, 52, 53]. The value of d for various fields (corresponding to the center of the segment from $H - \Delta H/2$ to $H + \Delta H/2$) was calculated in accordance with expression (4) from the model LAMS curves as

$$d = 4 - 2\Delta \ln(1 - M/M_s)/\Delta \ln(H).$$

The fractal dimension in Figs. 4 and 5 is shown as a function of l_H/l_g and l/l_g, respectively (l is the size of the region over which the fractal dimension is calculated in the BC method), which makes it possible to consider its physical meaning and to compare it with the results of determining the cluster dimension using the direct BC method (Fig. 5). First, Fig. 4 shows that in the range of scales for l_H exceeding particle size l_g, the fractal dimension passes to the regime in which it is almost independent of this scale. This indicates the statistical scale invariance of the studied magnetic structure for the given range of sizes and, hence, proves its fractal nature. The value of d corresponding to the plateau in Figs. 4 and 5 should be treated as an estimate of the dimension of the magnetic correlation volume (magnetic nonuniformity). Second, it can be seen that in the range of scales $1 < l_H/l_g < 2.5$, the fractal dimensions determined from the LAMS curves are in good agreement with the results obtained by the BC method (see Fig. 5). The fractal dimension of the film was found to be 2 (see Fig. 4), while for the Sierpinski carpet, it was $d = 1.81 \pm 0.02$, which is slightly lower than theoretical value $d = \ln 8/\ln 3 \approx 1.89$.

The fractal dimension of a cluster can be determined from the dependence of the coercive field on reduced particle size l_g/δ using Eq. (2), which means that $H_c \propto l_g^{2d/(4-d)}$. The value of H_c determined from the theoretical hysteresis loops for various ratios l_g/δ smaller than unity indeed demonstrates a power-law correlation of these parameters, $H_c \propto (l_g/\delta)^{\beta}$, in the case of fractal clusters with different dimensions (Fig. 6).

The fractal dimension calculated in this way is in good agreement with the dimension calculated using the BC method in the case when the dipole–dipole interaction is disregarded (Fig. 7). Fractal dimension d_{mag} estimated using Fig. 6b representing the results of

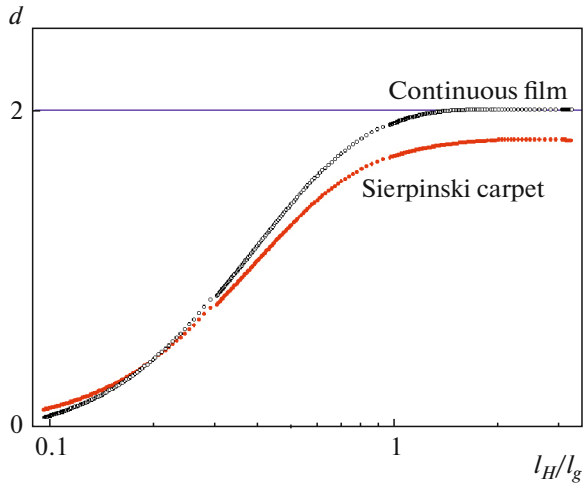

Fig. 4. (Color online) Fractal dimension obtained for the approach to the saturation magnetization for a continuous magnetic film and the Sierpinski carpet cluster.

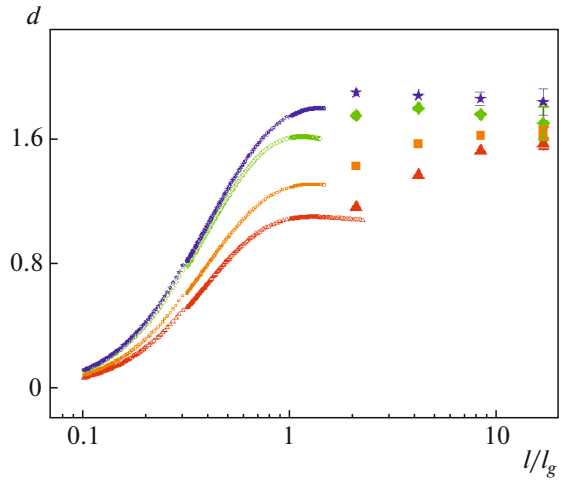

Fig. 5. (Color online) Fractal dimension d of 2D magnetic DLA clusters: (large symbols) data obtained by the BC method; (small symbols) LAMS data; (cluster *a*) blue stars; (cluster *b*) green diamonds; (cluster *c*) orange squares; (cluster *d*) red triangles.

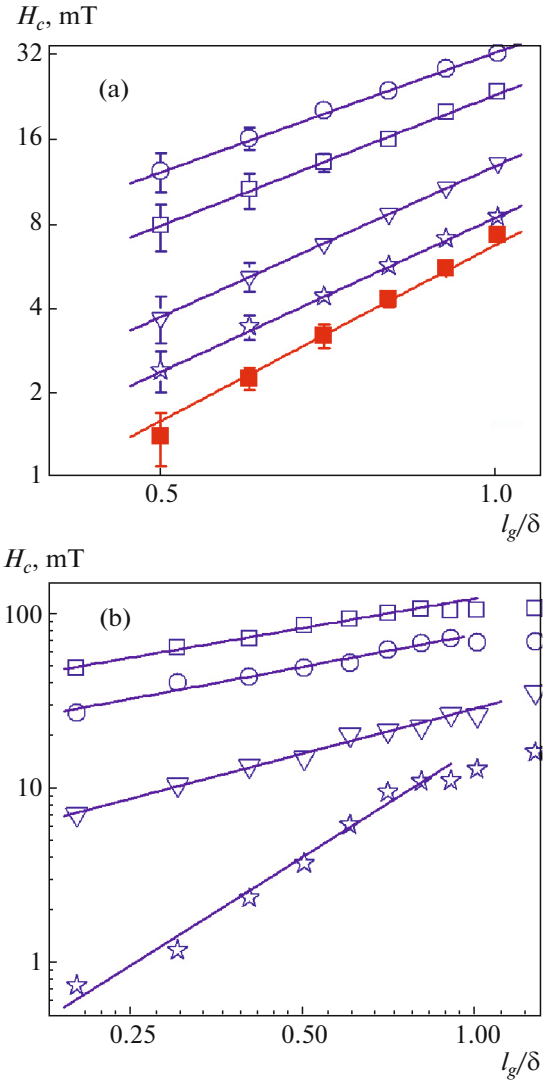

Fig. 6. (Color online) Dependence of the coercive field on the grain size (correlation radius of the easy magnetization axis) (a) disregarding and (b) taking into consideration of the dipole–dipole interaction: (solid squares) continuous magnetic film; (empty symbols) results for 2D magnetic DLA clusters; (circles) luster grown for particle adhesion probability $p = 1$; (squares) $p = 0.1$; (triangles) $p = 0.01$; and (stars) $p = 0.001$.

calculation of the dimensional dependences of the coercive field with allowance of the dipole–dipole interaction does not agree with the value of d_{bc} calculated using the BC method. The results obtained for different clusters are as follows: $d_{\text{mag}}/d_{bc} = (0.90 \pm 0.03)/(1.54 \pm 0.02)$ for cluster *a*; $(0.92 \pm 0.03)/(1.63 \pm 0.02)$ for cluster *b*; $(1.23 \pm 0.03)/(1.77 \pm 0.03)$ for cluster *c*, and $(2.01 \pm 0.03)/(1.91 \pm 0.02)$ for cluster *d* (see Fig. 1). Fractal dimension d_{mag} for clusters *a* and *b* is lower than physically substantiated limitation $d = 1$. Certain agreement for the *d*-type cluster with the highest density can be due to the fact that its structure is a continuous film with an insignificant concentration of pores. This situation was considered in detail in [54], which shows that the perturbation introduced into the magnetic microstructure by demagnetizing fields of a pore practically vanishes for pores with a small diameter ($l_g/\delta < 1$). Such a porous medium must behave (as regard its magnetic properties) as a defect-free and continuous medium. In our case, this must lead to observation with $d_{\text{mag}} = 2$, which is in full agreement with measured value $d_{\text{mag}} = (2.01 \pm 0.03)$. The final result (Fig. 7) shows that the fractal dimension of a cluster, which is obtained by the method of approach to saturation magnetization is in satisfactory agreement with the fractal dimension of this cluster determined by the BC method. It is important that the agreement is observed not only when the dipole–dipole interaction is disregarded, but also in the case when this interaction is accounted. Therefore, the method of fractal dimension measurement using the LAMS theory disregarding the dipole–dipole interaction gives reasonable estimates of d even for such complex objects as fractal magnetic clusters. The experimental values of noninteger fractal dimensions for nanogranular films and nanoporous media, which have been estimated earlier using this method [29, 30], are now additionally confirmed by numerical experiment.

It should be noted that reliable experimental estimates of the fractal dimension obtained using the LAMS method require the magnetization measurements in strong fields (from 0.1 to 10 T) with a high degree of accuracy (relative error is not smaller than 10^{-3}) [15, 45]. Modern vibration and SQUID magnetometers meet such requirements as a rule. Examples of successful practical application of this method can be found in [15, 26, 27].

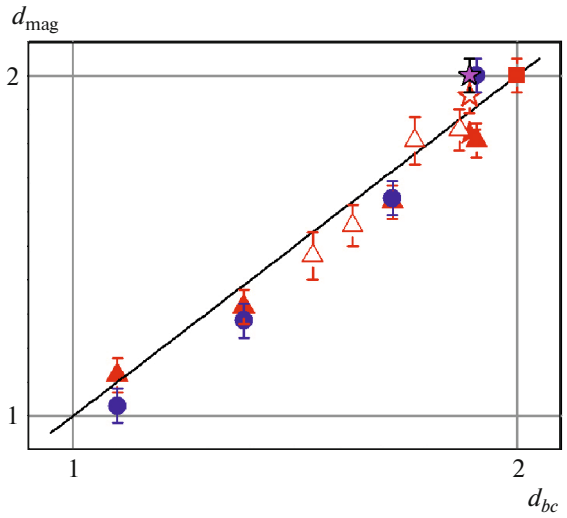

Fig. 7. (Color online) Correlation between the fractal dimension d_{bc} in a magnetic cluster, calculated using the BC method and fractal dimension d_{mag} calculated from magnetic properties; (filled symbols) data from analysis of the LAMS curve; (empty symbols) data from the dimensional dependence of the coercive field; (triangles) without the dipole–dipole interaction; (circles) with the dipole–dipole interaction correspond to DLA clusters; (stars) Sierpinski carpet; (squares) continuous film.

5. CONCLUSIONS

Numerical estimation of the reliability of experimental approaches to determining the magnetic microstructure dimension from magnetic properties for 2D fractal clusters of monodomain particles in the ground state has shown that the method for determining dimension from the LAMS curves, which was proposed earlier for such systems, can be considered as reliable. It turned out that the method of dimensional dependence of the coercive field in physically natural situations taking the dipole–dipole interaction between nanoparticles into consideration gives estimates of cluster dimension strongly differing from the estimates obtained using the BC method. This is due to considerable influence of the dipole–dipole interaction between nanoparticles in a fractal cluster in weak fields.

FUNDING

This work was supported by Russian Foundation for Basic Research, Government of Krasnoyarsk Territory, Krasnoyarsk Region Science and Technology Support Fund under the research project no. 18-42-240006.

REFERENCES

1. B. B. Mandelbrot, *The Fractal Geometry of Nature* (W. H. Freeman, US, 1982).
2. J. F. Gouyet, *Physics and Fractal Structures* (Springer, New York, 1996).
3. C. Swoboda, M. Martens, and G. Meier, Phys. Rev. B **91**, 064416 (2015).
4. P. Monceau and J.-C. S. Levy, Phys. Lett. A **374**, 1872 (2010).
5. S. H. Liu, Solid State Phys. **39**, 207 (1986).
6. T. Nakayama and K. Yakubo, *Fractal Concepts in Condensed Matter Physics* (Springer, Berlin, Heidelberg, 2003).
7. A. Bunde and S. Havlin, *Fractals and Disordered Systems* (Springer, Berlin, Heidelberg, 1996).
8. B. M. Smirnov, Sov. Phys. Usp. **29**, 481 (1986).
9. S. V. Karpov, V. S. Gerasimov, I. L. Isaev, and V. A. Markel, Phys. Rev. B **72**, 205425 (2005).
10. T. A. Witten and L. M. Sander, Phys. Rev. Lett. **47**, 1400 (1981).
11. M. Balasoiu, M. V. Avdeev, V. L. Aksenov, D. Hasegan, V. M. Garamus, A. Schreyer, D. Bica, and L. Vekas, J. Magn. Magn. Mater. **300**, e225 (2006).
12. A. V. Nagornyi, V. I. Petrenko, M. V. Avdeev, O. V. Yelenich, S. O. Solopan, A. G. Belous, A. Yu. Gruzinov, O. I. Ivankov, and L. A. Bulavin, J. Magn. Magn. Mater. **431**, 16 (2017).
13. G. Herzer, Mater. Sci. Eng. A **133**, 1 (1991).
14. R. S. Iskhakov, S. V. Komogortsev, A. D. Balaev, and L. A. Chekanova, JETP Lett. **72**, 304 (2000).
15. R. S. Iskhakov and S. V. Komogortsev, Phys. Met. Metallogr. **112**, 666 (2011).
16. V. A. Ignatchenko and V. A. Felk, Phys. Rev. B **71**, 094417 (2005).
17. V. A. Ignatchenko and V. A. Felk, Phys. Rev. B **74**, 174415 (2006).
18. V. A. Ignatchenko and V. A. Felk, Phys. Met. Metallogr. **100**, S63 (2005).
19. G. Herzer, IEEE Trans. Magn. **25**, 3327 (1989).
20. R. Skomski, J. Phys.: Condens. Matter **15**, R841 (2003).
21. G. Herzer, Acta Mater. **61**, 718 (2013).
22. R. S. Iskhakov, V. A. Ignatchenko, S. V. Komogortsev, and A. D. Balaev, JETP Lett. **78**, 646 (2003).
23. R. S. Iskhakov, S. V. Komogortsev, A. D. Balaev, A. V. Okotrub, A. G. Kudashov, V. L. Kuznetsov, and Yu. V. Butenko, JETP Lett. **78**, 236 (2003).
24. R. S. Iskhakov, S. V. Komogortsev, A. D. Balaev, and L. A. Chekanova, Tech. Phys. Lett. **28**, 725 (2002).
25. G. S. Kraynova, A. M. Frolov, and T. A. Pisarenko, Adv. Mater. Res. 718–720, 85 (2013).
26. R. S. Iskhakov, S. V. Komogortsev, B. A. Denisova, Yu. E. Kalinin, and A. V. Sitnikov, JETP Lett. **86**, 465 (2007).
27. S. V. Komogortsev, R. S. Iskhakov, A. A. Zimin, E. Y. Filatov, S. V. Korenev, Y. V. Shubin, N. A. Chizhik, G. Y. Yurkin, and E. V. Eremin, J. Magn. Magn. Mater. **401**, 236 (2016).
28. R. S. Iskhakov, S. V. Komogortsev, A. D. Balaev, and A. A. Gavriliuk, J. Magn. Magn. Mater. **374**, 423 (2015).
29. V. A. Ignatchenko and R. S. Iskhakov, Fiz. Met. Met. **73**, 602 (1992).

30. E. M. Chudnovsky, W. M. Saslow, and R. A. Serota, Phys. Rev. B **33**, 251 (1986).
31. D. A. Garanin, E. M. Chudnovsky, and T. Proctor, Phys. Rev. B **88**, 224418 (2013).
32. V. A. Ignatchenko and R. S. Iskhakov, Izv. Akad. Nauk SSSR, Ser. Fiz. **44**, 1434 (1980).
33. V. A. Ignatchenko, R. S. Iskhakov, and G. V. Popov, Sov. Phys. JETP **55**, 878 (1982).
34. G. Herzer, in *Handbook of Magnetism and Advanced Magnetic Materials*, Ed. by H. Kronmüller and S. S. P. Parkin (Wiley, Hoboken, 2007).
35. R. S. Iskhakov and S. V. Komogortsev, Bull. Russ. Acad. Sci.: Phys. **71**, 1620 (2007).
36. A. Michels, R. N. Viswanath, J. G. Barker, R. Birringer, and J. Weissmuller, Phys. Rev. Lett. **91**, 267204 (2003).
37. A. Grob, S. Saranu, U. Herr, A. Michels, R. N. Viswanath, and J. Weissmuller, Phys. Stat. Sol. Appl. Res. **201**, 3354 (2004).
38. Y. Gao, D. Shindo, T. Bitoh, and A. Makino, Phys. Rev. B **67**, 172409 (2003).
39. I. R. McFadyen and I. A. Beardsley, J. Appl. Phys. **67**, 5540 (1990).
40. V. I. Petrov, G. V. Spivak, and O. P. Pavlyuchenko, Sov. Phys. Usp. **15**, 66 (1972).
41. T. Suzuki, Phys. Status Solidi **37**, 101 (1970).
42. H. W. Fuller and M. E. Hale, J. Appl. Phys. **31**, 238 (1960).
43. J. Echigoya, J. Mater. Sci. **40**, 3209 (2005).
44. S. Thomas, S. H. Al-Harthi, D. Sakthikumar, I. A. Al-Omari, R. V. Ramanujan, Y. Yoshida, and M. R. Anantharaman, J. Phys. D **41**, 155009 (2008).
45. S. V. Komogortsev and R. S. Iskhakov, J. Magn. Magn. Mater. **440**, 213 (2017).
46. P. Garoche and A. P. Malozemoff, Phys. Rev. B **29**, 226 (1984).
47. J. Rampe, Visions of Chaos, Vol. 59.3, 2016. http://softology.com.au/voc.htm.
48. M. J. Donahue and D. G. Porter, 1999 OOMMF User's Guide, Vers. 1.0, Interagency Report NISTIR No. 6376 (2004).
49. S. V. Komogortsev, V. A. Fel'k, R. S. Iskhakov, and G. V. Shadrina, J. Exp. Theor. Phys. **125**, 323 (2017).
50. S. V. Komogortsev and R. S. Iskhakov, Phys. Solid State **47**, 480 (2005).
51. W. Maass, U. Krey, and H. Hoffmann, Phys. Statud Solidi **122**, K137 (1984).
52. V. Dupuis, J. P. Perez, J. Tuaillon, V. Paillard, P. Melinon, A. Perez, B. Barbara, L. Thomas, S. Fayeulle, and J. M. Gray, J. Appl. Phys. **76**, 6676 (1994).
53. L. Thomas, J. Tuaillon, J. P. Perez, V. Dupuis, A. Perez, and B. Barbara, J. Magn. Magn. Mater. 140–144, 437 (1995).
54. E. Schlomann, J. Appl. Phys. **38**, 5027 (1967).

Translated by N. Wadhwa